arXiv:1611.07598v2 [cond-mat.dis-nn] 21 Dec 2016

Wave Transport and Intensity inside Disordered One-Dimensional Systems: Single-Parameter Scaling and Maximum-Entropy. Theory and Experiment.

Xiaojun Cheng,[1] Azriel Z. Genack,[1] Xujun Ma,[1] Pier A. Mello,[2] and Miztli Yépez[3]

[1]*Department of Physics, Queens College and the Graduate Center of the City University of New York, Flushing, NY, 11367 USA*
[2]*Instituto de Física, Universidad Nacional Autónoma de México, Ap. Postal 20-364, 01000 México, D. F., Mexico*
[3]*Departamento de Física, Universidad Autónoma Metropolitana-Iztapalapa, A. P. 55-534, 09340 México D. F., Mexico*

The single-parameter scaling hypothesis relating the average and variance of the logarithm of the conductance is a pillar of the theory of electronic transport and classical wave propagation. We extend random-matrix theory into the interior of one-dimensional random samples using a maximum-entropy ansatz to study the statistics of particle and energy density. We find that the average of the logarithm of the energy density at a depth x is equal to $-x/\ell$, where ℓ is the mean free path. These results are in accord with microwave measurements and computer simulations.

PACS numbers: 71.55.Jv,71.23.-k,41.20.Jb, 84.40.-x

Studies of electronic transport have focused on the scaling of the conductance. Many of the predictions of mesoscopic physics and localization theory apply equally to the transport of classical waves and electronic transport, via the identification of the transmittance, T, with the conductance expressed in units of the quantum of conductance [1–8]. It is often difficult to carry out electronic measurements in ensembles of statistically equivalent disordered samples, but this can readily be done for classical waves. This has enabled detailed comparison of theory and measurements of the statistics of transport of classical waves (Ref. [7]).

The intensity of waves inside a random system has long been studied (see, e.g., Refs. [9–11]). Recently, the intensity distribution inside random systems has been explored using a weak-localization correction to the diffusion equation [12] to yield a position-dependent diffusion coefficient, $D(x)$, which is progressively renormalized with increasing depth into the sample. Solving a generalized diffusion equation with a position dependent diffusion coefficient gives the intensity profile inside random systems. For deeply localized samples, a supersymmetry approach beyond the single-loop approximation has provided an exact expression for $D(x)$ and the intensity profile that is confirmed in simulations [13]. Interest in the intensity profile inside random media has intensified recently because of the possibility of measuring the transmission matrix [14, 15] and of controlling waves transmitted through and in the interior [16–23] of random systems by preparing the incident wave in specific transmission eigenchannels.

A key assumption in the theory of wave transport is that the scaling and statistics of the transport depend upon a single parameter. The single parameter scaling (SPS) hypothesis holds that the distribution of the logarithm of the conductance or transmittance is a Gaussian with variance equal to twice the magnitude of the average transmittance [24], $\mathrm{var}(\ln T) = -2\langle \ln T\rangle$. Here, $\langle\cdots\rangle$ indicates the average over statistically equivalent samples. SPS has aided in understanding the statistics at the output surface. It is interesting to consider the possible extension of this result to fluctuations of particle or energy density inside the medium.

In this Letter we study the statistics of particle and energy density in the interior of 1D random samples, using random-matrix theory within a maximum-entropy approach (MEA) [25]. We find a strikingly simple extension of SPS, $\langle \ln \mathcal{W}(x)\rangle = -x/\ell$, where $\mathcal{W}(x)$ is the energy density at depth x normalized so that its value at the sample output is T, ℓ being the elastic mean free path (mfp). The probability distribution function of $\ln \mathcal{W}(x)$ is Gaussian away from the sample input with its variance increasing linearly with depth x from the sample input boundary until it begins to fall near the output surface. These results are confirmed in microwave measurements and computer simulations in random single-mode waveguides.

The MEA presented in Ref. [25] is a random-matrix theory which gives rise to a Fokker-Planck equation, known as the Dorokhov-Mello-Pereyra-Kumar (DMPK) equation [26, 27], governing the "evolution" with sample length L of the probability distribution function (pdf) $p_L(M)$ of the system *transfer matrix* M. The concept of transfer matrix is particularly useful due to its multiplicativity property. In the MEA, the disordered system is assumed to contain a large number of very weak scatterers: the dense-weak-scattering limit (DWSL). In the MEA, an *ansatz* is proposed for the pdf of the transfer matrix for a thin piece of material, a "building block", which contains the physical information relevant to the problem. It is expected that in the DWSL the MEA give results largely independent of the microscopic details.

The DMPK equation was developed for N (propagating) modes. For one dimension (1D), the DMPK equation [27] reduces to the Melnikov equation [4], introduced earlier than DMPK. The use of Melnikov's equation to study the statistical properties of the intensity profile inside random 1D samples was initiated in Ref. [28], where

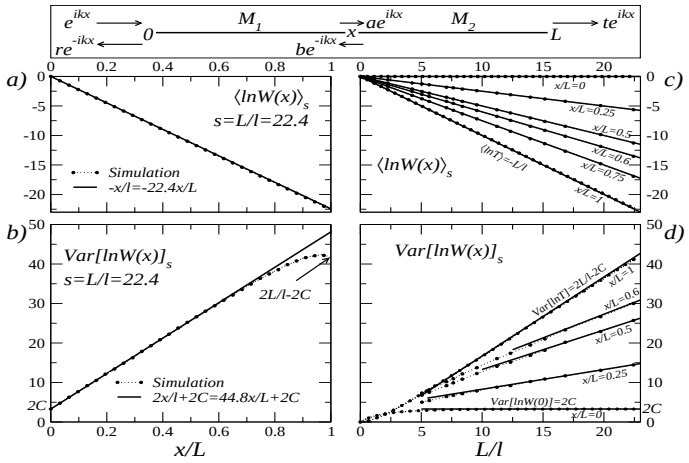

FIG. 1: The scattering problem associated with the 1D disordered waveguide of length L described in the text is illustrated in the top part of the figure. Theoretical results (full lines) and computer simulations (circles and dotted lines) for the profiles $\langle \ln \mathcal{W}(x) \rangle_s$ and $\mathrm{var}[\ln \mathcal{W}(x)]_s$ are shown, as functions of x/L, for fixed $s = L/\ell$, in panels (a) and (b), respectively. For the variance, Eq. (12) was complemented with Eq. (13) when $x = L$, as shown by the arrow: their combination accounts for the bending of the curve shown by the simulation. The same quantities are shown as functions of s for a few fixed values of x/L in the right panels, (c) and (d): we see clearly how they extend to the internal region of the sample the results for $\langle \ln T \rangle_s$ and $\mathrm{var}[\ln T]_s$. In panel (c), the agreement is excellent in all cases. In panel (d) the agreement is excellent for $s_2 \gg 1$. Computer simulations consist of 10^5 realizations and the parameters $kd = 0.1$ and $k\ell = 178$ were used.

the expectation value of the energy density inside the 1D sample, $\mathcal{W}(x)$, was obtained and compared successfully with computer simulations. In the present paper, we extend this analysis to investigate the statistics of the self-averaging quantity $\ln \mathcal{W}(x)$. These studies may provide a path for extending the analysis to quasi-1D disordered systems supporting more than one open channel.

Consider the scattering by a 1D random distribution of scatterers, as illustrated in the top part of Fig. 1. This situation may arise: i) in a Quantum Mechanical (QM) problem describing electronic scattering in a disordered conductor, or ii) in the problem of an electromagnetic (EM) wave in a disordered waveguide supporting a single transverse mode, or of a plane wave impinging upon a random layered medium. Indicated in Fig. 1 are the amplitudes of the incident, transmitted and reflected waves at either end of the waveguide. A small gap is opened at the point x inside the sample, where the amplitudes of the waves travelling to the right and left are shown. The transfer matrices M_1, M_2 of the two parts of the sample are also indicated.

The intensity inside the gap between the segments, normalized so that $\mathcal{W}(L) = T$, is

$$\mathcal{W}(x) = |ae^{ikx} + be^{-ikx}|^2. \tag{1}$$

We write the transfer matrices of the two portions of the waveguide as

$$M_i = \begin{bmatrix} \alpha_i & \beta_i \\ \beta_i^* & \alpha_i^* \end{bmatrix}, \qquad i = 1, 2, \tag{2}$$

with the condition $|\alpha_i|^2 - |\beta_i|^2 = 1$, thus satisfying the requirements of time-reversal invariance and flux conservation. When no index i is employed, the various quantities refer to the wire as a whole. The intensity given in Eq. (1) is expressible as [28]

$$\mathcal{W}(x) \equiv \mathcal{W}(x; M_1, M_2) = \frac{|\alpha_2^* e^{ikx} - \beta_2^* e^{-ikx}|^2}{|\alpha_2 \alpha_1 + \beta_2 \beta_1^*|^2} \equiv T F_x(M_2) \,, \tag{3}$$

where k denotes the wavenumber and $T(M_1, M_2)$ the transmission coefficient of the full sample. In the polar decomposition defined in Ref. [25], the transfer matrices M_i can be written in terms of "radial parameters" λ_i $[T_i = 1/(1+\lambda_i)]$ and two phases, θ_i and μ_i, as $\alpha_i = \sqrt{1+\lambda_i}\exp(i\theta_i)$, $\beta_i = \sqrt{\lambda_i}\exp(i(2\mu_i - \theta_i))$. In terms of these parameters, the function $F_x(M_2)$ appearing in Eq. (3) takes the form

$$F_x(M_2) = 1 + 2\lambda_2 - 2\sqrt{\lambda_2(1+\lambda_2)}\cos(2(\mu_2 - \theta_2 + kx)) \,. \tag{4}$$

The above expressions refer to a single configuration of disorder. Assuming the disorder is uncorrelated, the various quantities associated with the two sections that form the full sample are statistically independent of one another. The expectation value over an ensemble of configurations of a function $f(\mathcal{W}(x))$ can be computed using the pdf of the transfer matrices for the two sections of the waveguide, $p_x(M_1)$ and $p_{L-x}(M_2)$, respectively. The Melnikov equation governs the evolution with L of the marginal pdf of the radial parameter $\lambda \geq 0$ as

$$\frac{\partial w_s(\lambda)}{\partial s} = \frac{\partial}{\partial \lambda}\left[\lambda(1+\lambda)\frac{\partial w_s(\lambda)}{\partial \lambda}\right] \,. \tag{5}$$

Here, $s = L/\ell$ is the sample length in units of the mfp. The diffusion equation (5) is solved with the initial condition $w_{s=0}(\lambda) = \delta_+(\lambda)$, where $\delta_+(\lambda)$ is a one-sided delta function. In what follows, the statistics of the radial parameters λ_1, λ_2 of the two statistically independent sections of the wire will be described by Eq. (5): for the left segment of the sample, s will be replaced by $s_1 = x/\ell$, and for the right segment, by $s_2 = (L-x)/\ell$.

From Eq. (3) we find

$$\langle \ln \mathcal{W}(x) \rangle = \langle \ln T \rangle_{L/\ell} + \langle \ln F_x(M_2) \rangle_{(L-x)/\ell} \,. \tag{6}$$

The first term is given by the well-known expression

$$\langle \ln T \rangle_{L/\ell} = -L/\ell \equiv -s \,. \tag{7}$$

The second term has the structure

$$\langle \ln F_x(M_2)\rangle_{(L-x)/\ell}$$
$$= \Big\langle \ln\big[A(\lambda_2) - B(\lambda_2)\cos(2(\mu_2-\theta_2+kx))\big]\Big\rangle_{s_2} \quad (8a)$$
$$= \int_0^\infty d\lambda_2 \int_0^{2\pi} d\theta_2 w_{s_2}(\lambda_2,\theta_2)\int_0^{2\pi}\frac{d\mu_2}{2\pi}$$
$$\times \ln\big[A(\lambda_2) - B(\lambda_2)\cos(2(\mu_2-\theta_2+kx))\big] \quad (8b)$$
$$= (L-x)/\ell \equiv s_2, \quad (8c)$$

where we used Eq. (4.224.9) of Ref. [30] to evaluate the angular integral in Eq. (8b). The final result is

$$\langle \ln \mathcal{W}(x)\rangle = -\frac{x}{\ell}. \quad (9)$$

For $x = L$, this reduces to Eq. (7) for the full sample.

From Eq. (3), the second moment of $\ln \mathcal{W}(x)$ can be written as

$$\Big\langle [\ln \mathcal{W}(x)]^2\Big\rangle = \quad \big\langle (\ln T)^2\big\rangle_{L/\ell} + \Big\langle [\ln F_x(M_2)]^2\Big\rangle_{(L-x)/\ell}$$
$$+2\Big\langle (\ln T)\,[\ln F_x(M_2)]\Big\rangle . \quad (10)$$

Although we have not succeeded in computing the quantities occurring in Eq. (10) for an arbitrary value of L/ℓ, we have found approximate expressions for the case when the right segment of the sample is localized, $s, s_2 \gg 1$. For the three terms in Eq. (10) we obtain

$$\big\langle (\ln T)^2\big\rangle_{L/\ell} = s^2 + 2s - 2C + \omega_1(s), \quad (11a)$$
$$\Big\langle [\ln F_x(M_2)]^2\Big\rangle_{s_2} = s_2^2 + 2s_2 + \omega_2(s_2), \quad (11b)$$
$$2\Big\langle (\ln T)\,[\ln F_x(M_2)]\Big\rangle = -2s_2 s - 4s_2 + 4C + \omega_3(s_2), \quad (11c)$$

where $C = \int_0^\infty \langle T\rangle_s ds = 1.64493\cdots$, and $\omega_i(s)$ are functions that tend to 0 as $s \to \infty$. Collecting terms and using the result (9) we find, for the variance of $\ln \mathcal{W}(x)$,

$$\mathrm{var}\,[\ln \mathcal{W}(x)] = 2\frac{x}{\ell} + 2C + \omega(s_2), \quad s, s_2 \gg 1. \quad (12)$$

For $x = L$ we cannot apply the above result, Eq. (12), since this would violate the condition $s_2 \gg 1$. Since for $x = L$, $\mathcal{W}(L) = T$, one finds, from Eqs. (11a) and (7)

$$(\mathrm{var}(\ln T))_{L/\ell} = 2\frac{L}{\ell} - 2C + \omega_1(s), \quad s \gg 1\,. \quad (13)$$

The first term of Eq. (13) represents the well-known result that the variance of the logarithm of the transmission scales as twice (the absolute value of) its expectation value. In addition, to this order, $\ln T$ has a normal probability distribution with the above centroid and variance [24, 29]. The next term in Eq. (13), i.e., $-2C$, is of order s^0; it does not violate SPS, since it is a constant independent of the system parameters. To the best of our knowledge, this correction had not been reported before: earlier studies were restricted to lowest order in s; here we see that this term is not negligible even if $s \gg 1$.

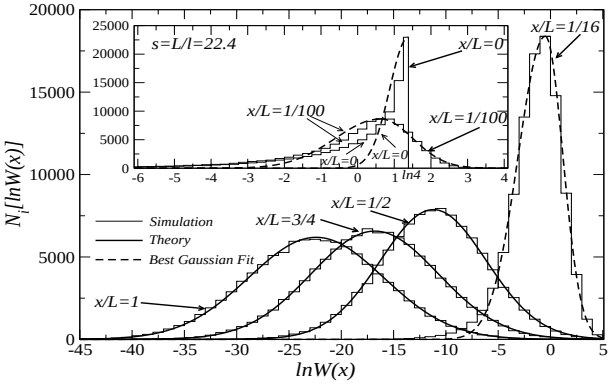

FIG. 2: Evolution of the statistical distribution of $\ln \mathcal{W}(x)$ for $x/L = 1.0,\ 3/4,\ 1/2$ and $1/16$, the first value corresponding to $\ln T$. The histograms are the results of computer simulations, the number of realizations being 10^5 for every histogram. We used the parameters $kd = 0.1$ and $k\ell = 178$. All cases are well inside the localized regime, as $s = L/\ell = 22.4$. The ordinate gives the number of events N_i that fall in box i of the histogram, so that $\sqrt{N_i}$ gives, approximately, the statistical error bar arising from the finiteness of the sample. The continuous curves are Gaussians with the parameters discussed in the text. When x is not too close to zero, the agreement between the theoretically constructed Gaussians and the computed generated histograms is excellent.

To check results, we have carried out computer simulations for samples supporting a single propagating mode. These simulations can be applied to both the QM and EM cases: i) in the QM case, the disordered potential is a random function of position; we chose sequences of equidistant barriers (idealized as delta-function potentials), with separation d small compared with the wavelength; ii) in the EM case, it is the index of refraction n appearing in the Helmholtz equation which is a similar random function of position.

The profile of $\langle \ln \mathcal{W}(x)\rangle_s$ and $\mathrm{var}[\ln \mathcal{W}(x)]_s$, Eqs. (9) and (12), are shown, as functions of x/L, for given s, in panels a) and b) of Fig. 1. Since Eq. (12) is not valid too close to the right end of the sample, it has to be substituted by Eq. (13) when $x = L$, as indicated in the figure. Computer simulations are seen to be in excellent agreement with theoretical results. Notice from Eq. (12) that the theoretical value for $x = 0$ is a *universal* result in the localized regime, which agrees with simulation.

The first moment and variance of $\ln \mathcal{W}(x)$ are shown as functions of s for fixed values of x/L in panels c) and d), respectively. They show the way that SPS continues in the interior of the sample.

We have not succeeded in finding the pdf of $\ln \mathcal{W}(x)$ analytically, but only numerically (Fig. 2): i) When x is not too close to 0, e.g. for $x/L = 3/4$ and $1/2$, $\ln \mathcal{W}(x)$ has a normal pdf with the theoretical centroid and vari-

ance given in Eqs. (9) and (12). When $x/L = 1$, the pdf is normal, with $\langle \ln \mathcal{W}(L) \rangle = -s$ and $\mathrm{var}[\ln \mathcal{W}(L)]_s = \mathrm{var}[\ln T]_s$, Eq. (13). ii) For $x = 0$, unitarity restricts $\ln \mathcal{W}(0) \leq \ln 4$ (inset in Fig. 2). The pdf cannot be fitted by a truncated Gaussian: see the dashed curve which is the best "half-Gaussian" fit (with the maximum at $\ln 4$) to the histogram. iii) When $x \neq 0, L$, unitarity imposes no restriction on $\ln \mathcal{W}(x)$. Very close to the left end of the sample, $x/L \ll 1$, the pdf of $\ln \mathcal{W}(x)$ admits non-zero values for $\ln \mathcal{W}(x) > \ln 4$. iv) For $x/L = 1/16$ (body of the figure) and $1/100$ (inset), the dashed curves show the best fit to the histograms given by two "half-Gaussian" distributions on the RHS and LHS of the maximum, achieved with two different sets of parameters; however, the left tail is longer than the Gaussian fit.

We have carried out microwave experiments to explore the statistics of $\ln \mathcal{W}(x)$ inside a random single-mode waveguide. Since $\ln \mathcal{W}(x)$ self-averages, we are able to obtain sufficient sampling to compare the measurements to theoretical predictions in 100 random configurations. Waves are launched from one end of the waveguide and the signal is detectied by an antenna above a slit along the length of the waveguide. The sample is composed of randomly positioned elements contained within a WR-90 rectangular copper waveguide, with width and height 2.286 cm and 1.016 cm, and cutoff frequency 6.56 GHz. The sample is a dielectric ceramic material with dielectric constant $\epsilon = 15$, of thickness 0.66 cm, covering 93% of the cross section of the waveguide, and a thin U-shaped Teflon which is essentially air. Each element in each random configuration has an equal chance of being either a dielectric or air layer. Thickness of the air layers is randomly selected from 1.275, 2.550, or 3.825 cm. The incident frequency ranges from 8.50 GHz to 8.59 GHz in 400 frequency steps. The total length of the sample is 60 cm. Absorption is removed by Fourier transforming into the time domain and with the factor $e^{\Gamma_a t/2}$ and transforming back into the frequency domain; $\Gamma_a = 0.011$ ns^{-1} is the decay rate of energy within the sample due to absorption and leakage through the slit along the sample length. It is obtained from the measurement of the linewidth in angular frequency units of the narrowest mode when copper reflectors are placed at the ends of the sample with only a small opening in the reflector at the LHS of the sample to admit energy from the source antenna.

The experimental results for $\langle \ln \mathcal{W}(x) \rangle$ shown in Fig. 3a are well fit by the line $5.06x/L + 0.02$. This linear behavior is in agreement with the fit $s = L/\ell \approx 5$ and $\ell \approx 12$ cm. The $\mathrm{var}(\ln \mathcal{W}(x))$ is shown in Fig. 3b: it increases linearly near the beginning of the sample and bends as x approaches the output boundary, as in the theoretical result of Fig. 1b). However, $\mathrm{var}(\ln \mathcal{W}(0)) \sim 5$ is larger than the predicted value of $2C = 3.29$. This is a consequence of reflection by the source antenna. We find in 1D simulations for a layered sample with an initial layer with a high value of index of refraction n_r, and

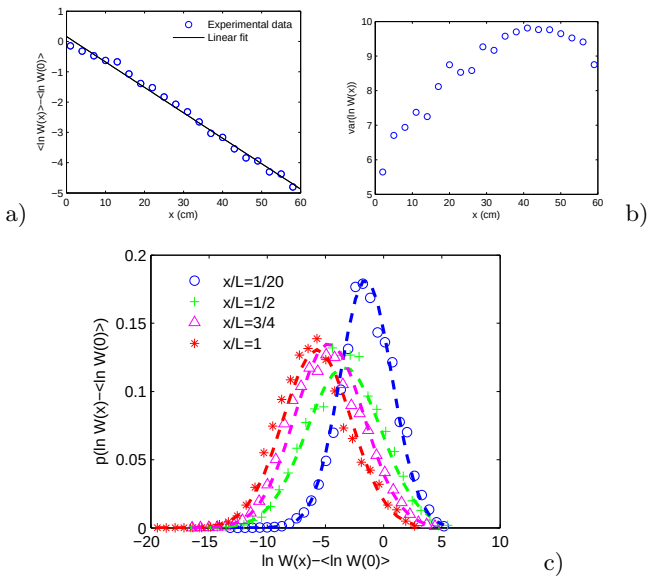

FIG. 3: Results from microwave experiments for (a) $\langle \ln \mathcal{W}(x) \rangle$, (b) $\mathrm{var}(\ln \mathcal{W}(x))$. The solid line in (a) shows comparison to the theoretical prediction of a linear fall-off as in Eq. (9). (c) The experimental results for the pdf of $\ln \mathcal{W}(x)$ at different locations for $s = 5$. The lines are Gaussian fit curves.

hence of reflectivity, that the slope of $\langle \ln \mathcal{W}(x) \rangle$ is not affected by reflection from the boundary, but $\mathrm{var}(\ln \mathcal{W}(0))$ increases with n_r. The pdf of $\ln \mathcal{W}(x)$ is shown in Fig. 3c. At the beginning of the sample the distribution is not symmetric; the fit shown in Fig 3c utilizes different Gaussian functions above and below the maximum value. However, for $x = L/2$ and $x = L$, the pdfs for $\ln \mathcal{W}(x)$ are Gaussian functions as seen in Fig. 3c. These results are consistent with features seen in Fig. 2.

In summary, we have used random-matrix theory to extend the study of the statistics of $\ln T$ into the interior of random 1D samples by calculating the statistics of $\ln \mathcal{W}(x)$, thus generalizing the SPS theory. Results are in excellent agreement with numerical simulations of wave propagation in a single-mode waveguide with scattering layers. For $\langle \ln \mathcal{W}(x) \rangle$ we find the simple relation of Eq. (9). This remarkable linearity is maintained, even in samples in which part of the wave is reflected into the sample and in samples with residual structural correlation in which the local density of states falls inside the samples. Extending the MEA into the interior of 1D samples provides a starting point for analyzing the intensity inside systems supporting several open modes.

The authors are indebted to B. Shapiro for valuable suggestions. PAM and AG wish to thank the Israel Institute of Technology (Haifa, Israel), where part of this work was started, for its hospitality. PAM acknowledges support by DGAPA under contract No. IN109014, and AZG the support of the National Science Foundation under grant No. 1609218 and of Noel Evans and Howard

Rose for constructing the experimental assembly.

[1] D. J. Thouless, Phys. Rev. Lett. **39**, 1167 (1977).
[2] E. Abrahams, P. Anderson, D. C. Licciardello, and T. V. Ramakrishnan, Phys. Rev. Lett. **42**, 673 (1979).
[3] P. W. Anderson, D. J. Thouless, E. Abrahams, and D. S. Fisher, Phys. Rev. B **22**, 3519 (1980).
[4] V. I. Mel'nikov, *Pis'ma Zh. Ekps. Teor. Fiz.* **32**, 244 (1980) [*JETP Lett.* **32**, 225 (1980)]; *Fis. Tverd. Tela (Leningrad)* **23**, 782 (1981) [*Sov. Phys. Solid State* **23**, 444 (1981)].
[5] O. N. Dorokhov, Solid State Commun. **51**, 381 (1984).
[6] M. C. W. van Rossum and T. M. Nieuwenhuizen, Rev. Mod. Phys. **71**, 313 (1999).
[7] Z. Shi, J. Wang, and A.Z. Genack, Proc. Nat. Ac. Sc. **111**, 2926 (2014).
[8] O. Dietz, U. Kuhl, H.-J. Stöckmann, N. M. Makarov, and F. M. Izrailev, Phys. Rev. B **83**, 134203 (2011).
[9] Y. L. Gazaryan, Sov. Phys. **29**, 996 (1969).
[10] W. Kohler and G. C. Papanicolau, J. Math. Phys. **14**, 1733 (1973).
[11] P. Neupane and A. G. Yamilov, Phys. Rev. B **92**, 014207 (2015).
[12] B. A. van Tiggelen, A. Lagendijk, and D. S. Wiersma, Phys. Rev. Lett. **84**, 4333 (2000); S. E. Skipetrov and B. A. van Tiggelen, Phys. Rev. Lett. **96**, 043902 (2006).
[13] C. Tian, S. Cheung, and Z. Zhang, Phys. Rev. Lett. **105**, 263905 (2010).
[14] I. M. Vellekoop and A. P. Mosk, Phys. Rev. Lett. **101**, 120601 (2008).
[15] S. M. Popoff, G. Lerosey, R. Carminati, M. Fink, A. C. Boccara, and S. Gigan, Phys. Rev. Lett. **104**, 100601 (2010).
[16] W. Choi, A. P. Mosk, Q. Park, and W. Choi, Phys. Rev. B **83**, 134207 (2011).
[17] B. Gérardin, J. Laurent, A. Derode, C. Prada, and A. Aubry, Phys. Rev. Lett. **113**, 173901 (2014).
[18] S. Liew, S. Popoff, A. P. Mosk, W. L. Vos, and H. Cao, Phys. Rev. B **89**, 224202 (2014).
[19] A. G. Yamilov, R. Sarma, B. Redding, B. Payne, H. Noh, and H. Cao, Phys. Rev. Lett. **112**, 023904 (2014).
[20] R. Sarma, A. Yamilov, P. Neupane, B. Shapiro, and Hui Cao, Phys. Rev. B **90**, 014203 (2014).
[21] M. Davy, Z. Shi, J. Wang, X. Cheng, and A. Z. Genack, Phys. Rev. Lett. **114**, 033901 (2015).
[22] M. Davy, Z. Shi, J. Park, C. Tian, and A. Z. Genack, Nat. Commun. **6**, 6893 (2015).
[23] R. Sarma, A. Yamilov, P. Neupane, and H. Cao, Phys. Rev. B **92**, 180203(R) (2015).
[24] C. W. J. Beenakker, Rev. Mod. Phys. **69**,731 (1997).
[25] P. A. Mello and N. Kumar, *Quantum Transport in Mesoscopic Systems* (Oxford University Press, 2010.)
[26] O. N. Dorokhov, Pis'ma Zh. Eksp. Teor. Fiz., **36**, 259 (1982) [JETP Lett., **36**, 318 (1982)]
[27] P. A. Mello, P. Pereyra, and N. Kumar, Ann. Phys. (NY) **181**, 290 (1988).
[28] P. A. Mello, Z. Shi, and A. Genack, Physica E **74** 603 (2015).
[29] P. A. Mello, J. Math. Phys. **27**, 2876 (1986).
[30] I. S. Gradshteyn and I. M. Ryzhik, *Table of Integrals, Series, and Products* (Academic Press, New York and London, 1965.)